Improving PSS performance of Srepok 3 hydropower plant using parameter optimization

Tran Van Dung[1*], Nguyen Hoang Mai[2], Nguyen Doan Phuoc[3]

[1]*Dak Lak College*
[2]*University of Science and Technology - The University of Danang*
[3]*HaNoi University of Science and Technology*
[*]*Corresponding author E-mail: tranvandungcdn@gmail.com*
DOI: https://doi.org/10.64032/mca.v30i4.402

Abstract

This paper presents a study on improving the damping performance of a supplementary stabilizing controller for a hydropower generating unit at the Srepok 3 hydropower plant. The excitation system, including the Automatic Voltage Regulator (AVR) and stabilizing feedback, is modeled using a linearized single-machine infinite-bus (SMIB) representation with actual plant parameters. The uncontrolled system exhibits low-frequency oscillations caused by insufficient damping. To isolate the influence of the stabilizer gain, the conventional washout and lead-lag PSS in (8) is replaced in the small-signal model by the explicitly stated reduced-order law $V_{PSS} = K_{STAB}.\Delta\omega$. This gain-only model is not dynamically equivalent to a complete PSS because it omits frequency-dependent magnitude and phase compensation. An eigenvalue-based parametric search is then used to determine K_{STAB} by minimizing the deviation between system eigenvalues and desired pole locations. Simulation results for the reduced-order model indicate that the optimized gain reduces the settling time from approximately 2 *s* to 1.4 *s* and attenuates oscillations. The results establish the effect of gain tuning for the considered model, while implementation with a complete PSS requires reintroduction of the dynamic filters and subsequent retuning and validation.

Keywords: *Hydropower Plants; Excitation System; AVR; PSS; Generator; Optimal Controller*

Symbol

E_t	*V*	Generator terminal voltage
V_t	*V*	Excitation voltage
V_{ref}	*V*	Reference voltage
T_M	-	Mechanical torque
T_e	-	Electrical torque
T_D	-	Damping torque
K_D	-	Damping coefficient
K_A	-	AVR gain
K_{STAB}	-	PSS gain
H	*s*	Inertia constant
ω	*rad/s*	Rotor rotation speed
$\Delta\omega$	*rad/s*	Rotor speed deviation
δ	*rad*	Rotor angle (load angle)
T'_{d0}	-	Open-circuit field time constant
T_R	-	Voltage transducer time constant
$G_{PSS}(s)$	-	PSS transfer function

Abbreviations

AVR	Auto Voltage Regulator
PSS	Power System Stabilizer
EXS	Excitation System
SMIB	Single-Machine Infinite-Bus

1. Introduction

Power system stability is essential for the secure, reliable, and efficient operation of modern electrical grids, particularly in large-scale generation systems such as hydropower plants. In synchronous-generator-based power systems, the excitation system plays a crucial role in terminal voltage regulation and dynamic stability enhancement. The Automatic Voltage Regulator (AVR) adjusts the generator field excitation to maintain the terminal voltage close to its reference value. However, although a high-gain AVR can improve voltage regulation, it may also reduce the damping of electromechanical modes and contribute to low-frequency electromechanical oscillations [1], [2], [3].

Low-frequency oscillations, typically occurring in the range of 0.1–2 *Hz*, arise from the dynamic interaction between generator rotor and the external power network. If these oscillations are insufficiently damped, they may lead to sustained rotor-angle oscillations, reduced power transfer capability, increased mechanical stress, and even system instability [2], [4]. Therefore, small-signal stability analysis and damping controller design remain important tasks in power system operation and control. Among available analysis techniques, eigenvalue-based analysis is widely used to identify dominant oscillatory modes and assess damping performance in both single-machine and multi-machine power systems [2], [5].

A Power System Stabilizer (PSS) is commonly employed as a supplementary controller in the excitation system to enhance damping performance. By generating an additional stabilizing signal, usually derived from rotor speed deviation or electrical power variation, the PSS provides supplementary damping torque through the AVR input. Conventional PSS structures generally consist of a washout filter and lead–lag compensation blocks, whose parameters must be properly tuned to achieve adequate phase compensation and damping effectiveness [2], [6]. Standard

Received: 19 December 2025; Revised: 03 May 2026; Accepted: 16 July 2026.

excitation system and PSS models for stability studies are also recommended in IEEE Std 421.5-2016 [7].

Over the past decades, various PSS tuning strategies have been investigated, ranging from classical eigenvalue-sensitivity methods to wide-area damping control, online parameter estimation, robust control, and metaheuristic optimization [8], [9], [10], [11], [12]. These methods have demonstrated promising capability in improving damping performance under different operating conditions. Eigenvalue-sensitivity-based approaches provide a direct relationship between controller parameters and dominant oscillatory modes, while wide area damping controllers exploit remote measurements to improve inter-area oscillation damping [8], [9]. More recent studies have further explored online tuning and nature-inspired optimization algorithms to enhance PSS performance in modern power systems [10], [11], [12].

Despite these advances, many existing approaches require complex controller structures, multiple tuning parameters, or extensive validation on benchmark systems. Their practical implementation in existing hydropower plants may be constrained by excitation hardware and operational requirements. A gain-focused reduced-order study can therefore be useful as a preliminary analysis, provided that the omitted controller dynamics and the resulting limitations are stated explicitly.

Motivated by this practical requirement, this study focuses on optimizing the main stabilizer gain K_{STAB} from the eigenvalue distribution of the linearized generator–excitation system. The conventional PSS structure is retained as the physical reference in (8), whereas the simulations use the gain-only approximation in (9) to isolate the effect of feedback gain. This approximation does not preserve the complete PSS dynamics; the effects of the washout and lead-lag blocks are outside the scope of the reported results.

The proposed method is applied to the Srepok 3 Hydropower Plant in Vietnam, which has a total installed capacity of 220 *MW*. The generator–excitation system is modeled using a linearized SMIB representation with actual plant parameters. The system is first analyzed without stabilizing feedback and then with the reduced-order gain-only controller. The stabilizer gain is selected by minimizing the deviation between the closed-loop eigenvalues and the desired pole locations.

The main contributions of this paper are summarized as follows:

- A linearized generator–excitation system model is developed using actual parameters from the Srepok 3 Hydropower Plant;
- The low-frequency oscillatory behavior of the system is investigated using eigenvalue-based small-signal stability analysis;
- An explicit closed-loop matrix $A_{PSS}(K_{STAB})$ is derived from the plant matrix A and the AVR reference-input channel, enabling transparent eigenvalue-guided gain tuning;
- The effectiveness of the optimized gain is evaluated through MATLAB/Simulink simulation and time-domain response analysis.

The remainder of this paper is organized as follows. Section 2 presents the generator–excitation system model and the SMIB-based state-space formulation. Section 3 describes the PSS structure and the eigenvalue-based gain optimization method. Section 4 presents and discusses the simulation results. Finally, Section 5 concludes the paper and suggests future research directions.

2. Modeling of generator excitation system

2.1 Generator excitation system

The excitation system (EXS) provides the field current required to establish the magnetic field of a synchronous generator and plays a key role in regulating terminal voltage and maintaining system stability under varying load conditions. It typically consists of transformers, rectifiers, and an Automatic Voltage Regulator (AVR), which together supply and control the excitation voltage [2], [7].

In modern hydropower plants, static excitation systems using thyristor-controlled rectifiers are widely adopted due to their fast response and high reliability [7]. The AVR is the main control component of the excitation system. It adjusts the excitation voltage V_t to maintain the generator terminal voltage E_t close to the reference value V_{ref}.

Although the AVR improves voltage regulation, a high AVR gain may reduce system damping and lead to low-frequency electromechanical oscillations [1], [2]. This trade-off motivates the need for additional damping control mechanisms such as the Power System Stabilizer (PSS).

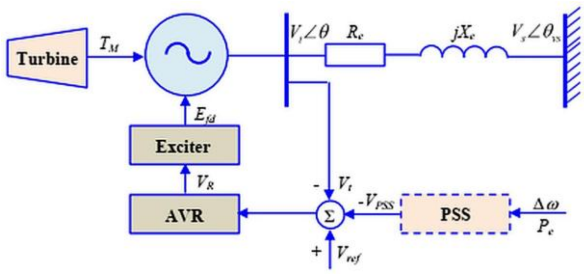

Figure 1: Single-machine infinite-bus (SMIB) system configuration.

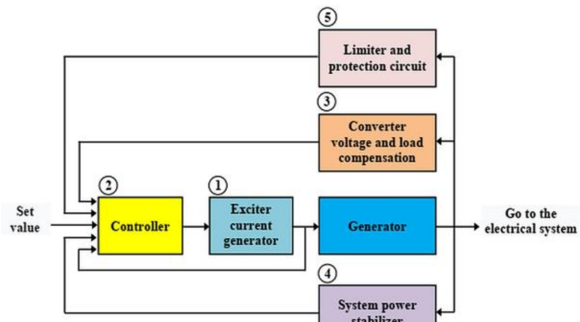

Figure 2: Excitation system (EXS) functional structure.

2.2 System modeling

The generator–excitation system is modeled using a linearized single-machine infinite-bus (SMIB) representation, which is widely used for small-signal stability analysis of power systems [2].

The SMIB model represents a synchronous generator connected to a large power system where the grid voltage and frequency are assumed constant. This allows the generator dynamics to be analyzed independently while preserving the essential characteristics of electromechanical oscillations.

From a physical perspective, the rotor dynamics are governed by the swing equation [2], [4]:

$$2H\frac{d\Delta\omega}{dt} = T_M - T_e - K_D\Delta\omega \tag{1}$$

where H is the inertia constant, T_M is the mechanical torque, T_e is the electrical torque, and K_D is the damping coefficient.

For small disturbances around the operating point, the electrical torque T_e can be linearized as:

$$\Delta T_e = K_1\Delta\delta + K_2\Delta E_q \tag{2}$$

where K_1 is the synchronizing torque coefficient and K_2 represents the coupling between electrical torque and internal voltage.

Substituting (2) into (1) yields:

$$2H\frac{d\Delta\omega}{dt} = T_M - K_1\Delta\delta - K_2\Delta E_q - K_D\Delta\omega \tag{3}$$

This formulation establishes a direct relationship between rotor motion and electrical variables, forming the basis for state-space modeling.

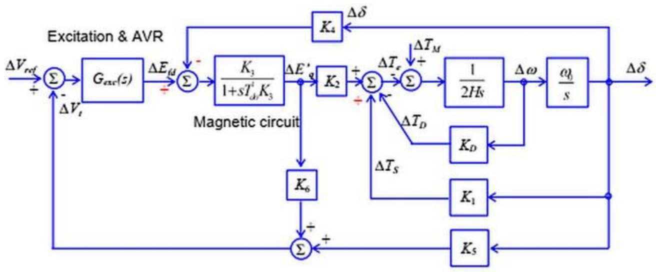

Figure 3: Linearized block diagram of the generator and excitation system.

The system dynamics are described by the rotor angle δ, angular speed ω, internal voltage E_q, and excitation voltage E_{fd}. By linearizing the nonlinear system around an operating point, the model can be expressed in state-space form:

$$\dot{x} = Ax + Bu \tag{4}$$

where

$$x = \left[\Delta\delta, \Delta\omega, E_q, E_{fd}\right]^T,\ u = \left[T_M, V_{ref}\right]^T \tag{5}$$

Based on the linearized block diagram (Fig. 3), the system matrix is obtained as:

$$A = \begin{bmatrix} 0 & K\omega & 0 & 0 \\ -K_f K_1 & -K_f K_D & -K_f K_2 & 0 \\ -\dfrac{K_4}{T'_{d0}} & 0 & -\dfrac{1}{T'_{d0}K_3} & -\dfrac{K_A}{T'_{d0}} \\ \dfrac{K_5}{T_R} & 0 & \dfrac{K_6}{T_R} & -\dfrac{1}{T_R} \end{bmatrix} \tag{6}$$

where $K_f = \dfrac{1}{2H}$ represents the inverse of the inertia constant, and $K_\omega = 1$ denotes the direct relationship between rotor speed deviation and rotor angle dynamics. K_3 represents a scaling factor introduced during the linearization process to account for the interaction between internal voltage and field dynamics.

$$B = \begin{bmatrix} 0 & 0 \\ K_f & 0 \\ 0 & \dfrac{K_A}{T'_{d0}} \\ 0 & 0 \end{bmatrix} \tag{7}$$

The parameters used in the model are obtained from the actual Srepok 3 hydropower plant at the selected nominal operating point and are summarized in Table 1.

The coefficients K_1–K_6 are operating-point-dependent gains obtained by linearizing the Heffron–Phillips model. Table 1 reports the single coefficient set used to construct the nominal matrix A and to perform the simulations in Section 4. In particular, K_1 contributes to synchronizing torque, K_D represents damping effects, and K_A governs the excitation-system gain [2].

Table 1: Parameters of the excitation and generator systems at the nominal operating point

Parameter	Value	Parameter	Value
K_1	0.7636	K_A	200
K_2	0.8644	T_A	3
K_3	0.3231	K_D	12
K_4	1.4189	T'_{d0}	7.29
K_5	-0.1463	T_R	0.02
K_6	0.4167	H	3.6

Note: $K_5 = -0.1463$ is the fixed value at the nominal operating point used in (6) and in the simulations. Figure 5 shows values recalculated after relinearizing the model at other active-power levels.

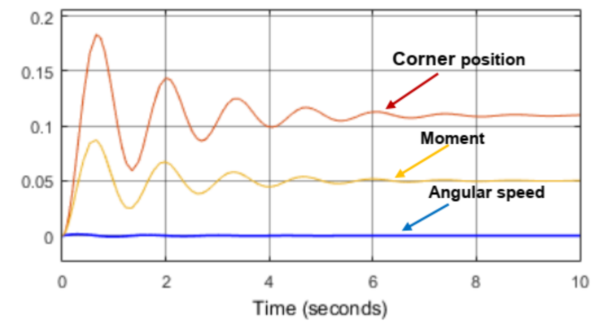

Figure 4: System response under a 5% disturbance with positive K_5.

The matrix A represents the linearized dynamics of the generator–excitation system. Its elements capture the interaction between rotor motion, electrical torque, and excitation dynamics. Increasing excitation gain improves voltage regulation but may reduce damping by shifting eigenvalues toward the imaginary axis.

The model described in (6), (7) corresponds to the generator–excitation system without a Power System Stabilizer (PSS). System stability is evaluated through eigenvalue analysis of the matrix A. Eigenvalues located close to the imaginary axis indicate low damping and result in oscillatory behavior.

This baseline model serves as the foundation for the control design presented in the next section, where the system is extended by incorporating the PSS and modifying the system dynamics accordingly.

3. PSS modeling and parameter optimization

3.1 Analysis of excitation system characteristics

To understand the dynamic behavior of the generator–excitation system, the influence of key system parameters is analyzed under different operating conditions.

Fig. 4 shows the system response under a small disturbance. The presence of sustained oscillations indicates insufficient inherent damping in the excitation system.

Fig. 5 presents an operating-point sweep rather than a parameter that varies during one simulation. At each normalized active-power level, the nonlinear model is relinearized and a new value of K_5 is calculated. The value $K_5 = -0.1463$ in Table 1 is the fixed nominal operating-point value used to construct A in (6) and in all simulations reported in Section 4.

Fig. 6 presents the variation of the damping torque coefficient. It can be observed that damping capability is not constant and may decrease under certain loading conditions.

Fig. 7 shows the variation of the synchronizing torque coefficient, which is essential for maintaining rotor angle stability. A reduction in this coefficient may lead to increased oscillatory behavior.

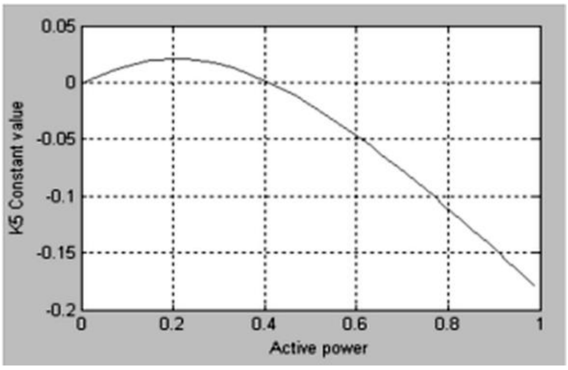

Figure 5: Operating-point dependence of K_5 obtained by relinearization over the active-power sweep.

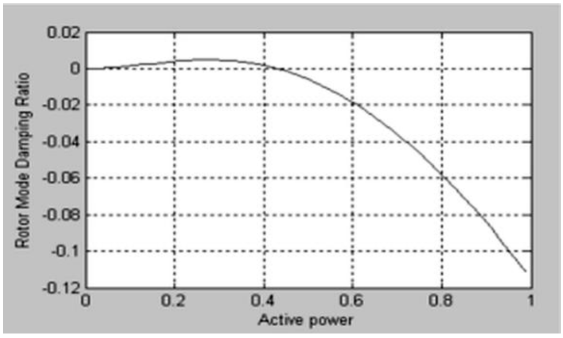

Figure 6: Variation of damping (quenching) torque coefficient with active power.

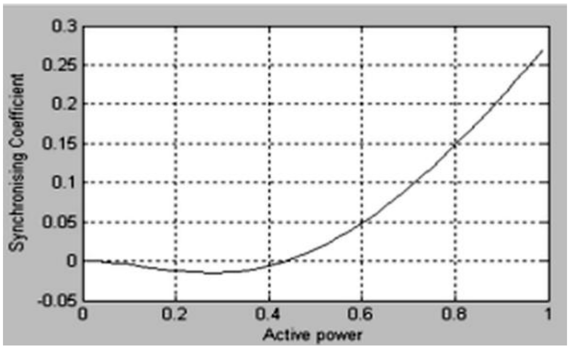

Figure 7: Variation of synchronizing torque coefficient with active power.

These results indicate that the intrinsic damping characteristics of the generator–excitation system depend strongly on the operating point. Nevertheless, every individual linear simulation uses one fixed coefficient set. Analysis at a different loading condition requires relinearization and reconstruction of the matrix A before the PSS gain is evaluated.

3.2 PSS structure and integration

To enhance system damping, a Power System Stabilizer (PSS) is introduced as a supplementary control input to the AVR in Fig. 8. The conventional PSS receives rotor-speed deviation and generates an additional signal at the AVR summing junction. Its complete dynamic structure, including the washout and lead-lag blocks, is shown in Fig. 9.

The conventional dynamic transfer function of the PSS is given by [2], [7]:

$$G_{PSS}(s) = K_{STAB} \cdot \frac{sT_W}{1+sT_W} \cdot \frac{1+sT_1}{1+sT_2} \tag{8}$$

Equation (8) represents the complete washout and lead-lag dynamics. In the present study, only the gain effect is analyzed, and the controller is deliberately reduced to:

$$V_{PSS} = K_{STAB} . \Delta\omega \tag{9}$$

The law in (9) is a reduced-order approximation and is not dynamically equivalent to the conventional PSS in (8). Omitting the washout and lead-lag blocks removes their frequency-dependent attenuation and phase compensation and reduces the controller order. This choice is made solely to isolate the influence of K_{STAB} on the dominant small-signal eigenvalues and to obtain a transparent closed-loop matrix. Consequently, the optimized gain and the time-domain results reported below apply only to the gain-only model. Direct implementation in a complete PSS requires restoring the dynamic blocks, followed by retuning and validation.

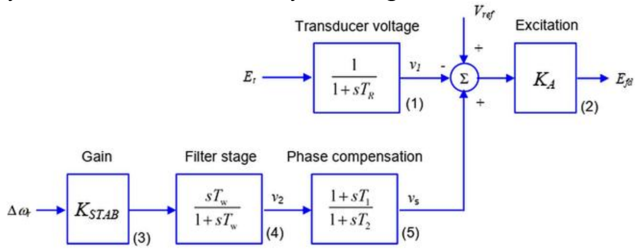

Figure 8: Static excitation system with AVR and PSS.

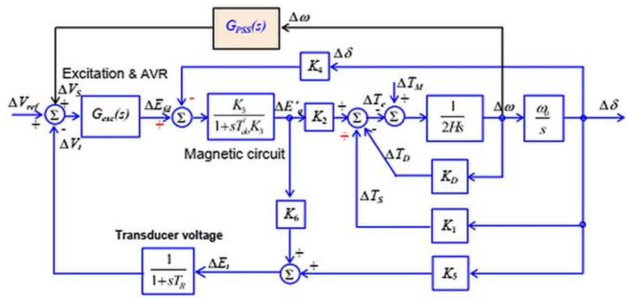

Figure 9: Structure of the Power System Stabilizer (PSS).

3.3 Eigenvalue-based gain optimization

Define $C_\omega = [0 \quad 1 \quad 0 \quad 0]$, so that $\Delta_\omega = C_\omega x$, and let b_v denote the second column of B in (7), $b_v = [0 \;\; 0 \;\; K_A/T'_{d0} \;\; 0]$^$T$, corresponding to the AVR reference-input channel. With the positive summing convention in Fig. 8, $\Delta V_{ref.eff} = \Delta V_{ref} + V_{PSS}$. Substitution of (9) into (4) gives:

$$\dot{x} = A_{PSS}(K_{STAB})x + Bu, \quad A_{PSS} = A + b_V . K_{STAB} . C_\omega \tag{10}$$

$$A_{PSS}(K_{STAB})=\begin{bmatrix} 0 & K\omega & 0 & 0 \\ -K_fK_1 & -K_fK_D & -K_fK_2 & 0 \\ -\frac{K_4}{T'_{d0}} & \frac{K_A.K_{STAB}}{T'_{d0}} & -\frac{1}{T'_{d0}K_3} & -\frac{K_A}{T'_{d0}} \\ \frac{K_5}{T_R} & 0 & \frac{K_6}{T_R} & -\frac{1}{T_R} \end{bmatrix} \quad (11)$$

Equation (11) follows directly from the outer product $b_v.K_{STAB}.C_\omega$. Relative to A in (6), only element (3,2) changes by $+K_AK_{STAB}/T'_{d0}$; all other entries remain unchanged. If the PSS signal is implemented with the opposite summing sign, the same derivation applies with the corresponding negative sign. This explicit construction also shows why the gain-only approximation preserves the four plant states, whereas a complete washout/lead-lag PSS would require additional controller states and an augmented system matrix.

The damping performance of the system can be evaluated using the damping ratio:

$$\xi=\frac{-\mathrm{Re}(\lambda)}{\sqrt{\mathrm{Re}(\lambda)^2+\mathrm{Im}(\lambda)^2}} \quad (12)$$

where the damping ratio is defined for complex conjugate eigenvalues representing oscillatory modes. To improve system stability, the stabilizer gain is optimized such that the system eigenvalues are shifted toward a region associated with higher damping.

$$J(K_{STAB})=\|\lambda(A_{PSS}(K_{STAB}))-\lambda_d\|_2 \quad (13)$$

$$K^*_{STAB}=\arg\min_{K_{STAB}} J(K_{STAB}) \quad (14)$$

where λ_d is a desired eigenvalue vector representing improved damping characteristics.

In this study, the optimal gain is obtained using a parametric search over a predefined range of K_{STAB}, evaluating the objective function for each candidate value.

This approach provides a practical alternative to more complex optimization-based PSS tuning methods reported in recent literature [10], [11], [12], [13], while maintaining implementation simplicity.

With in the gain-only model, the effect of K_{STAB} can be interpreted directly from the sensitivity of the eigenvalues of $A_{PSS}(K_{STAB})$. Increasing the gain may shift the dominant eigenvalues toward the left half-plane and increase the damping ratio; however, excessive gain may also reduce robustness or destabilize another mode. This interpretation is not automatically transferable to the complete PSS in (8), whose filter states introduce additional poles, zeros, and phase effects.

Therefore, the optimization problem in (14) aims to balance damping improvement and system stability, ensuring that the dominant modes are sufficiently damped without introducing instability.

3.4 Discussion

The analysis demonstrates that system damping depends on both the operating point and the excitation-system parameters. The reduced-order stabilizing feedback provides a transparent way to study the influence of one gain and to derive $A_{PSS}(K_{STAB})$ explicitly. Its simplicity results from restricting the model scope, not from claiming dynamic equivalence with a complete PSS. The optimized value must therefore be regarded as an initial gain for subsequent validation using the full washout and lead-lag dynamics.

4. Simulation results and discussion

4.1 Simulation setup and response analysis

The effectiveness of the proposed gain-tuning method is evaluated using a MATLAB/Simulink model of the generator–excitation system. The plant is implemented from the state-space formulation in Section 2, and the supplementary feedback is incorporated according to the reduced-order law in (9). No washout or lead-lag controller states are included in these simulations.

The system parameters are obtained from the Srepok 3 hydropower plant at the nominal operating point (Table 1). Accordingly, K_5 is fixed at −0.1463 throughout the simulations; the curve in Fig. 5 is used only to illustrate how a new linearization would change K_5 at another loading condition.

To excite the system dynamics, a step disturbance is applied to the mechanical torque T_M, creating an imbalance between mechanical and electrical torque. This disturbance induces electromechanical oscillations, which are used to evaluate the damping performance of the system.

Three operating scenarios are considered:

- Case 1: System without PSS;
- Case 2: System with a selected fixed gain in the reduced-order law (9);
- Case 3: System with the optimized gain in the reduced-order law (9).

The corresponding time-domain responses are shown in Figs. 10–12.

Without PSS, the system exhibits sustained low-frequency oscillations with slow decay, indicating insufficient inherent damping.

With a selected fixed gain in (9), the oscillation amplitude is reduced and the system stabilizes more quickly. However, residual oscillations are still present, indicating that the selected gain does not provide the best damping for the nominal model.

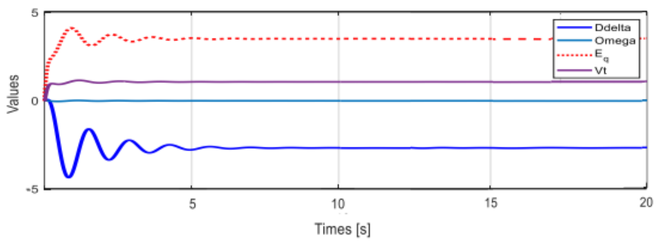

Figure 10: System response without PSS.

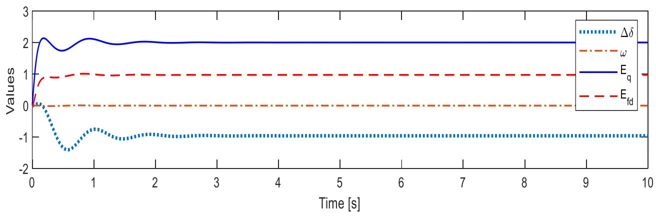

Figure 11: System response with a selected fixed gain in the reduced-order model.

With the optimized gain in the reduced-order model, the system response is significantly improved. Oscillations are rapidly attenuated, and the system reaches steady state in a shorter time. This confirms the effectiveness of the eigenvalue-guided gain selection for the nominal gain-only model introduced in Section 3.

4.2 Quantitative evaluation and discussion

The performance of the system under different configurations is summarized in Table 2.

To further illustrate the effectiveness of the proposed method, the dominant eigenvalues of the system under different configurations are analyzed.

The results demonstrate a clear improvement in system performance as the gain-only feedback is refined. The optimized gain reduces the settling time by approximately 30% compared with the uncontrolled case and significantly enhances the damping characteristics of the nominal model.

From an eigenvalue perspective, the improvement in time-domain response can be explained by the shift of the dominant poles toward the left half-plane. Without supplementary feedback, the eigenvalues are located close to the imaginary axis, resulting in low damping. The selected fixed gain produces a moderate shift, whereas the optimized gain moves the dominant eigenvalues further left and yields faster oscillation decay.

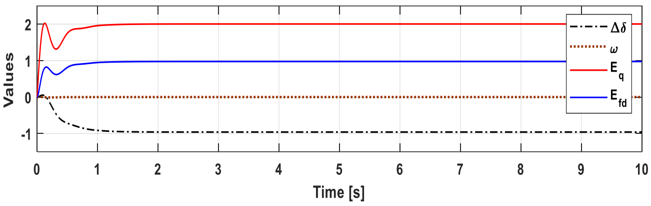

Figure 12: System response with the optimized gain in the reduced-order model.

These results are consistent with the analysis presented in Section 3, where the stabilizer gain is tuned to guide the system eigenvalues toward a region associated with improved damping.

Table 2: Performance comparison of the gain-only feedback configurations based on time-domain response and damping characteristics

Metric	No PSS	Fixed gain	Optimized gain
Settling time (s)	2.0	1.7	1.4
Peak overshoot	High	Medium	Low
Oscillation decay rate	Slow	Moderate	Fast
Damping level	Low	Medium	High

Overall, the study confirms that eigenvalue-based gain tuning can improve the dynamic response of the nominal generator–excitation model. The result should not be interpreted as validation of a complete PSS implementation because the washout and lead-lag dynamics are absent from (9). Those blocks can alter phase compensation, introduce additional modes, and change the optimal gain. Robustness across operating points and validation with the complete PSS model remain necessary before practical deployment.

5. Conclusion

This paper has presented an eigenvalue-based approach for selecting the gain of a reduced-order supplementary stabilizing controller for the Srepok 3 hydropower plant excitation system. A linearized SMIB model was developed using plant parameters at a selected nominal operating point. The uncontrolled system exhibited low damping, while the gain-only feedback in (9) improved the dominant small-signal response. The conventional washout and lead-lag PSS structure was used as the physical reference, but its dynamic blocks were intentionally excluded from the simulation model; therefore, the reported results are limited to the reduced-order representation.

Simulation results demonstrated that the optimized gain in the reduced-order model enhances damping, reduces oscillation amplitude, and shortens the settling time from approximately 2.0 s to 1.4 s. These results quantify the benefit of gain selection for the nominal model without claiming dynamic equivalence to a complete PSS.

The main contribution of this work lies in establishing an explicit relationship between K_{STAB} and the closed-loop matrix, $A_{PSS} = A + b_v.K_{STAB}.C_\omega$, and in using this relationship for systematic eigenvalue-guided gain selection. The manuscript also distinguishes the nominal value $K_5 = -0.1463$ used in the simulations from the operating-point sweep shown in Fig. 5.

The results confirm that a transparent gain-only model can support preliminary damping studies without increasing controller complexity. Future work should restore the washout and lead-lag states, retune all PSS parameters, evaluate multiple operating points and uncertainties, and validate the resulting controller in a nonlinear multi-machine or real-time test environment.

References

[1] F. P. DeMello and C. Concordia, “Concepts of synchronous machine stability as affected by excitation control,” *IEEE Transactions on Power Apparatus and Systems*, vol. PAS-88, no. 4, pp. 316–329, 1969. DOI: 10.1109/TPAS.1969.292452.

[2] P. Kundur, *Power System Stability and Control*. New York, USA: McGraw-Hill, 1994.

[3] P. Kundur et al., “Definition and classification of power system stability,” *IEEE Transactions on Power Systems*, vol. 19, no. 3, pp. 1387–1401, 2004. DOI: 10.1109/TPWRS.2004.825981.

[4] P.W Sauer and M.A.Pai, *Power System Dynamics and Stability*. Wiley, 2017.

[5] M. Cheah-Mane et al., “A new paradigm for small-signal stability analysis in modern power systems: Challenges, models, and methods in power systems rich in power electronics,” *IEEE Power & Energy Magazine*, 2026. DOI: 10.1109/MPE.2025.3588485.

[6] S. S. Choi and X. M. Jia, “Coordinated design of under-excitation limiters and power system stabilizers,” *IEEE Transactions on Power Systems*, vol. 15, no. 3, pp. 937–944, 2000. DOI: 10.1109/59. 871716.

[7] IEEE Power and Energy Society, *Ieee recommended practice for excitation system models for power system stability studies*, IEEE, 2016. DOI: 10.1109/IEEESTD.2016.7553421.

[8] D. Sumina, I. Petrovic, and N. Peric, “Parameter tuning of power system stabilizer using eigenvalue sensitivity,” *Electric Power Systems Research*, vol. 81, no. 12, pp. 2171–2177, 2011. DOI: 10.1016/j.epsr.2011.07.005.

[9] H. Wu, K. S. Tsakalis, and G. T. Heydt, “Evaluation of time delay effects to wide-area power system stabilizer design,” *IEEE*

Transactions on Power Systems, vol. 19, no. 4, pp. 1935–1941, 2004. DOI: 10.1109/TPWRS.2004.836272.

[10] D. Lauria, F. Mottola, G. Giannuzzi, C. Pisani, and S. Tessitore, "Power systems stabilizers online tuning based upon parameters dynamic estimation," *Sustainable Energy, Grids and Networks*, vol. 39, p. 101 481, 2024. DOI: 10.1016/j.segan.2024.101481.

[11] I. Hattabi, A. Chouder, M. A. Hannan, and H. Shareef, "Enhanced power system stabilizer tuning using marine predator algorithm with comparative analysis and real-time validation," *Scientific Reports*, vol. 14, p. 28 971, 2024. DOI: 10.1038/s41598-024-80154-2.

[12] C. Zhang, X. Chang, J. Dai, Z. Chen, and M. Babanezhad, "Designing of a wide-area power system stabilizer using an exponential distribution optimizer and fuzzy controller considering time delays," *Scientific Reports*, 2025. DOI: 10.1038/s41598-025-85524-y.

[13] D. Chitara et al., "Robust multi-machine power system stabilizer design using meta-heuristic optimization techniques," *International Journal of Electrical Power & Energy Systems*, 2024.